Development of in-situ sample cells for scanning transmission x-ray microscopy

Takuji Ohigashi, Masanari Nagasaka, Toshio Horigome, Nobuhiro Kosugi, Scott M. Rosendahl, and Adam P. Hitchcock

---

Articles you may be interested in

Scanning AC nanocalorimetry combined with in-situ x-ray diffraction
J. Appl. Phys. **113**, 243501 (2013); 10.1063/1.4811686

In-situ synchrotron x-ray transmission microscopy of the sintering of multilayers
Appl. Phys. Lett. **102**, 223107 (2013); 10.1063/1.4809602

In-situ X-ray diffraction combined with scanning AC nanocalorimetry applied to a Fe0.84Ni0.16 thin-film sample
Appl. Phys. Lett. **102**, 201902 (2013); 10.1063/1.4806972

In-situ observation of nickel oxidation using synchrotron based full-field transmission X-ray microscopy
Appl. Phys. Lett. **102**, 053902 (2013); 10.1063/1.4789991

NanoXAS—The in situ Combination of Scanning Transmission X-ray and Scanning Probe Microscopy
AIP Conf. Proc. **1365**, 449 (2011); 10.1063/1.3625399

Development of In-situ Sample Cells for Scanning Transmission X-ray Microscopy

Takuji Ohigashi[1, a)], Masanari Nagasaka[1], Toshio Horigome[1], Nobuhiro Kosugi[1], Scott M. Rosendahl[2] and Adam P. Hitchcock[3]

[1]*UVSOR Synchrotron, Institute for Molecular Science, 38 Nishigo-naka, Myodaiji, Okazaki, Aichi, 444-8585, Japan*
[2]*Canadian Light Source, 44 Innovation Boulevard, Saskatoon, SK S7N 2V3, Canada*
[3]*McMaster University, 1280 Main Street West, Hamilton, Ontario, L8S4L8, Canada*

a)Corresponding author: ohigashi@ims.ac.jp

Abstract. An azimuthal rotatable sample cell, an electrochemical cell and a controlled humidity cell for *in-situ* scanning transmission X-ray microscopy (STXM) were developed at UVSOR-III Synchrotron (Okazaki, Japan). By using these sample cells, the polarization dependence of sodium titanate nanoribbons, *in-situ* electrochemistry of 0.1M $FeSO_4$ solution, and *in-situ* morphological change of a functional polymer with changing humidity were successfully measured.

INTRODUCTION

In-situ spectromicroscopic measurements can reveal dynamics of morphological, physical and chemical processes. *In-situ* techniques have been developed for spectromicroscopic studies of heavy elements using hard X-rays with high transmittance in samples and long focal length of optical elements (i.e. long working distance) at photon energies >4 keV. On the other hand, *in-situ* measurements in the soft X-ray region for spectromicroscopic studies of light elements face significant technical challenges due to several difficulties, such as low transmittance and short focal lengths of optical elements. Scanning transmission X-ray microscopy (STXM) in the soft X-ray region is a promising technique for *in-situ* observation, considering its characteristics, such as high energy resolving power, high spatial resolution, low radiation damage and 2-dimensional (and 3-dimensional) chemical state analysis by using near edge X-ray absorption fine structure (NEXAFS). In UVSOR-III Synchrotron, Institute for Molecular Science (Okazaki, Japan), a STXM system was installed on the in-vacuum soft X-ray undulator beamline BL4U in 2012 and started user operation in 2013 [1]. Since then, we have been developing several types of sample cells and *in-situ* measurement methods to study soft matter such as polymer and biological systems. The sample cells described in this article are compatible with Bruker ASC (now, Research Instruments) STXM systems installed at SLS, BESSY-II, PLS, DLS, Soleil and so on.

NEW DESIGN OF A FRESNEL ZONE PLATE

One of the technical challenges for *in-situ* measurements by STXM is the very short working distance. A schematic of the optical system of STXM is shown in Fig. 1. The incoming X-rays are focused by a Fresnel zone plate (FZP) onto a sample through an order sorting aperture (OSA). The working distance is defined as the distance between OSA and the sample. In some *in-situ* sample cells described below (e.g. the electrochemical cell and the humidity control cell), a silicon nitride membrane (frame thickness of 200 μm) and a top cover plate (thickness of
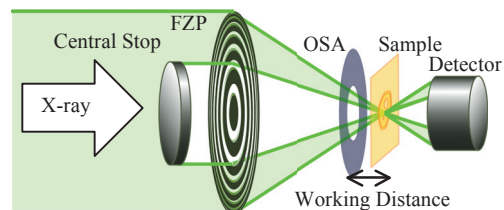

Fig. 1: Schematic of the optical system of STXM

050002-1

~100 µm) are used and additional clearance of 100 µm is needed for safety. To apply STXM of UVSOR-III Synchrotron to soft matter study, the C K-edge has to be covered as the lowest energy (i.e. condition of the shortest working distance) for the *in-situ* devices. In order to meet this requirement, a new FZP with the working distance more than 400 µm is required at 275 eV. Therefore, we have acquired a new FZP with outermost zone width of 35 nm, diameter of 240 µm and central stop diameter of 95 µm. By using the new FZP with an OSA of diameter of 65 µm, the working distance is >500 µm at the C K-edge.

AZIMUTHAL ROTATABLE SAMPLE CELL [2]

The absorption spectra of samples with anisotropic chemical bonding can show spectral changes as the polarization of the incoming linearly polarized X-rays is changed [3]. Samples with random orientations do not show polarization dependent X-ray absorption spectra. STXM can be used to measure polarized 2-dimensional maps of individual molecular orientations [4]. Typically, this kind of measurement is performed with a polarization tunable insertion device, such as an elliptical polarizing undulator. BL4U at UVSOR-III Synchrotron is equipped with an in-vacuum undulator which has fixed horizontal linear polarization. Therefore, we developed a sample cell which can rotate the sample azimuthally from outside of the STXM chamber. This cell is modeled on that reported by Hernández-Cruz et al [5]. A photo of the azimuthal rotatable sample cell (ARSC) is shown in Fig. 2. The ARSC uses a small stepping motor (AM1020, Faulhaber) to adjust the azimuthal angle of the sample.

Polarization dependent spectra of sodium titanate nanoribbons (STN) were measured using the ARSC. O 1s image sequences were obtained at several azimuthal angles. Figure 3a shows the azimuthal dependence of the O 1s spectrum of an individual nanoribbon, extracted from the same area of the sample (green rectangle in Fig. 3b). End member spectra corresponding to parallel and perpendicular orientation of the STN were extracted and used to fit the polarization dependent data, yielding a dichroic composite map (Fig. 3c).
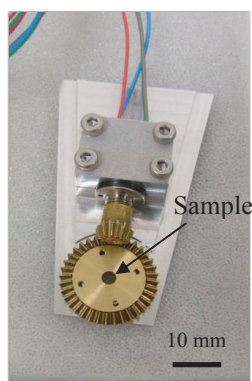

Fig. 2 Photo of the azimuthal rotatable sample cell
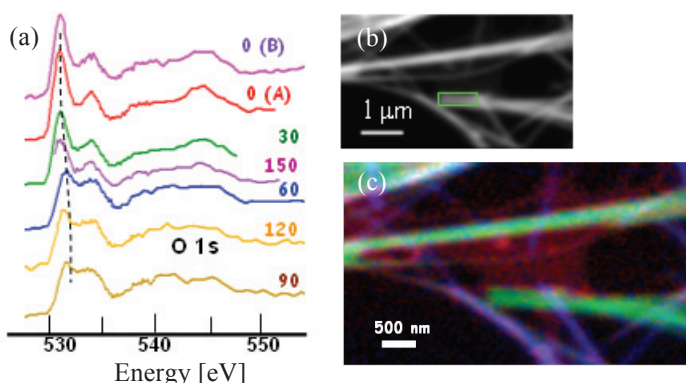

Fig. 3 (a) Angle dependence of the O 1s spectrum of the green highlighted STN. (b) Optical density image of several STN. (c) Color composite mapping (carbon support as red, parallel component as green and perpendicular component as blue)

ELECTROCHEMICAL CELL [6]

In-situ spectroscopic measurements of electro-chemical reactions have been performed widely using infrared [7], hard X-rays [8,9] and soft X-rays [10,11]. By using STXM, 2-dimensional distribution of electrochemical reactions occurring on or near electrodes can be analyzed with high spatial resolution. An important advance in this work relative to earlier electrochemical STXM studies [12,13] is that it is capable of continuous and interrupted flow of electrolytes, as opposed to previous systems which only used static (no-flow) conditions. The basic concept of a liquid flow cell
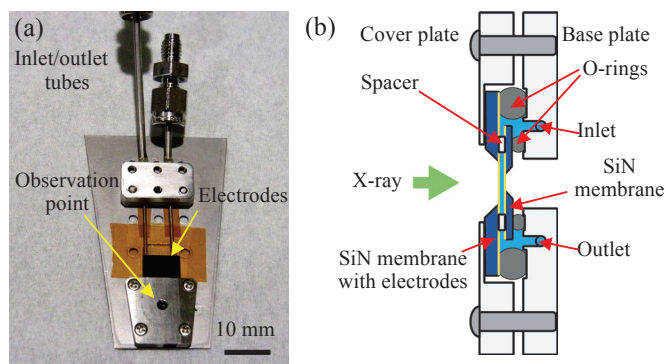

Fig. 4 (a) Photo and (b) cross sectional schematic of the electrochemical cell

050002-2

was developed by Nagasaka [14] and was modified for electrochemical experiments in the STXM. A photo and cross-sectional image of the electrochemical cell are shown in Fig. 4. The electrochemical cell consists of two silicon nitride membranes (thickness of 100 nm), teflon™ spacers (thickness of 20 μm) and two viton o-rings. The liquid electrolyte flows through a few micron gap between these membranes, driven by a peristaltic pump from outside of the STXM chamber via a fluidic feed through. The thickness of the gap can be optimized to get better contrast of target species by changing the pressure of helium gas in the STXM chamber. Three electrodes (50 nm thick gold with a Cr adhesion layer) - working (WE), counter (CE) and reference electrode (RE) - are deposited on the top (upstream) membrane. Electrical connections are made using a small home-made multi-pin connector.

By using this flow electrochemical cell, *in-situ* Fe 2p spectroscopy of the electrochemical reaction of an 0.1 M $FeSO_4$ aqueous solution was performed [6]. Figure 5a shows Fe 2p spectra of Fe(II) and Fe(III) measured in this system. These spectra were used to fit the Fe L_3-edge energy stack data to obtain component maps of Fe(II), Fe(III) and the electrodes (constant), from which a color coded composite is presented in Fig. 5b. In the composite map, the Fe(II)-rich region of the solution is in red, the Fe(III)-rich region is in green, and the gold electrodes (WE, CE and RE) are in blue. The distribution of Fe(III) and Fe(II) was opposite from our expectation since the WE was positive relative to the CE. These results are under investigation.
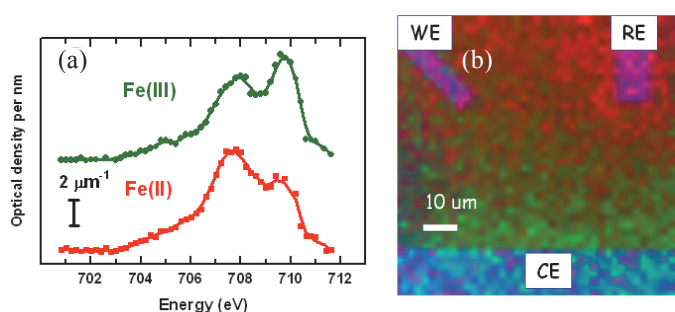

Fig. 5 (a) Fe(II) and Fe (III) spectra from an energy stack of 0.1 M $FeSO_4$ (aq) at 0 V (Fe(II)) and 0.6 V (Fe(III)). (b) Composite of component maps of Fe(II) in red, Fe (III) in green and the electrodes in blue.

HUMIDITY CONTROL CELL

A humidity control cell has been developed for *in-situ* measurements of the effects of water vapor on various materials [15-17]. The humidity control cell consists of a small chamber with two silicon nitride membranes for X-rays, a relative humidity (RH) sensor, and three ports for gas inlet/outlet (Fig. 6). The sample (polymer film on a TEM grid) is mounted on the top (upstream) silicon nitride membrane by scotch tape. By using the three ports for dry/wet gas inlet, the humidity in the sample cell is controlled by filling the cell with humid helium gas. Temperature and humidity inside the chamber are monitored by a small RH sensor (SHT7x, Sensirion AG) placed near the sample.

The effect of humidity on a thin section (100 nm) of a functional polymer was studied by changing the humidity *in-situ*. Figures 7a and 7b show STXM images of the polymer with 8 % and 84 % RH at room temperature, respectively. The images were taken with an X-ray energy of 285.5 eV and were converted to optical density. In these images, bright areas (i.e. high optical density) show high density regions of the polymer and dark areas (i.e. low optical density) show voids in the polymer. By changing the humidity from 8% to 84%, 8% of the dark area, for example shown in red circles in Figs. 7a and 7b, decreased. This change of the area was caused by swelling of the polymer as it absorbed water vapor.
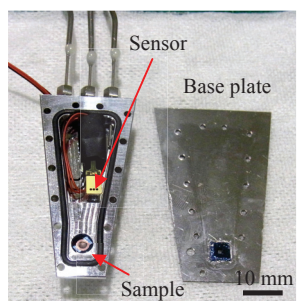

Fig. 6 Photo of the main chamber (interior) and the base plate of the humidity control sample cell.
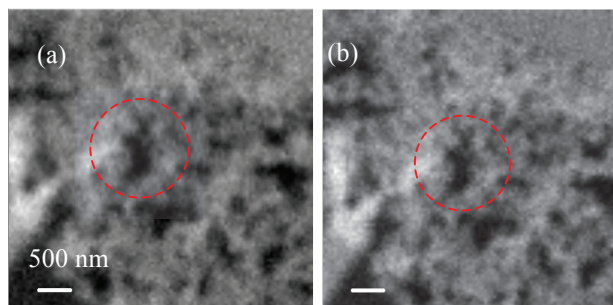

Fig. 7 Optical density images (285.5 eV) of a functional polymer at RH of (a) 8% , (b) 83%.

SUMMARY

We have developed *in-situ* measurement methods by designing and commissioning an azimuthal rotatable sample cell, an electrochemical cell, and a humidity control cell for chemical and biological applications of STXM. These sample cells and automated control systems are under further improvement. These *in-situ* measurement methods will allow users of the STXM to explore new fields in soft materials science. Access to the STXM in UVSOR-III Synchrotron is either by peer reviewed proposals twice a year, or by purchased access.

ACKNOWLEDGEMENTS

REFERENCES

1. T. Ohigashi, H. Arai, Y. Inagaki, N. Kondo, M. Sakai, K. Hayashi, E. Shigemasa, A. P. Hitchcock, N. Kosugi and M. Katoh, UVSOR Activity Report **40**, 43 (2013).
2. X. H. Zhu, T. Ohigashi, A. P. Hitchcock, C. Bittencourt, P. Umek and P. Krüger, UVSOR Activity Report **41**, 72 (2014).
3. J. Stöhr, *NEXAFS Spectroscopy*, (Springer, Berlin, 2003), pp. 169-172.
4. B. Watts, T. Schuettfort and C. R. McNeill, Adv. Funct. Mater. **21**, 1122-1131 (2011).
5. D. Hernández-Cruz, A.P. Hitchcock, T. Tyliszczak, M.-E. Rousseau and M. Pézolet, Rev. Sci. Instrum. **78**, 033703 (2007).
6. S. M. Rosendahl, A. P. Hitchcock, M. Nagasaka, Y. F. Wang, T. Horigome, T. Ohigashi and N. Kosugi, UVSOR Activity Report **42**, 117 (2015).
7. K. Ashley, S. Pons, Chem. Rev. **88**, 673−695 (1988).
8. T. Ohigashi, T. Aota, N. Watanabe, H. Takano, H. Yokosuka and S. Aoki, Jpn. J. Appl. Phys. **47**, 4742-4745 (2008).
9. A. Braun, S. Shrout, A. C. Fowlks, B. A. Osaisai, S. Seifert, E. Granlund and E. J. Cairns, J. Synchrotron Rad. **10**, 320-325 (2003).
10. M. Nagasaka, H. Yuzawa, T. Horigome, A. P. Hitchcock and N. Kosugi, J. Phys. Chem. C **117**, 16343-16348 (2013).
11. M. Nagasaka, H. Yuzawa, T. Horigome and N. Kosugi, Rev. Sci. Instrum. **85**, 104105 (2014).
12. D. Guay, J. Stewart-Ornstein, X. Zhang and A.P. Hitchcock, Anal. Chem. **77**, 3479-3487 (2005).
13. A. Gianoncelli, B. Kaulich, M. Kiskinova, C. Mele, M. Prasciolu, I. Sgura and B. Bozzini, J. Phys.: Conf. Ser. **425**, 182010 (2013).
14. M. Nagasaka, T. Hatsui, T. Horigome, Y. Hamamura and N. Kosugi, J. Electron Spectrosc. Relat. Phenom. **177**, 130-134 (2010).
15. T. Lefèvre, M. Pézolet, G. Cooper, D. H. Cruz, M. M. West, M. Obst, A. P. Hitchcock, C. Karunakaran and K. Kaznatcheev, J. Phys.: Conf. Ser. **186**, 012089 (2009).
16. T. Huthwelker, V. Zelenay, M. Birrer, A. Krepelova, J. Raabe, G. Tzvetkov, M. G. C. Vernooij and M. Ammann, Rev. Sci. Instrum. **81**, 113706 (2010).
17. J. Wang, J. Zhou, H. Fang, T.-K. Sham, C. Karunakaran, Y. Lu, G. Cooper and A. P. Hitchcock, J. Electron Spectrosc. Relat. Phenom. **184**, 296-300 (2011).